molecules

MDPI

Article

MR Study of Water Distribution in a Beech (*Fagus sylvatica*) Branch Using Relaxometry Methods

Urša Mikac [1], Maks Merela [2], Primož Oven [2], Ana Sepe [1] and Igor Serša [1,*]

[1] Department of Condensed Matter Physics, Jožef Stefan Institute, 1000 Ljubljana, Slovenia; urska.mikac@ijs.si (U.M.); ana.sepe@ijs.si (A.S.)
[2] Department of Wood Science and Technology, Biotechnical Faculty, University of Ljubljana, 1000 Ljubljana, Slovenia; maks.merela@bf.uni-lj.si (M.M.); primoz.oven@bf.uni-lj.si (P.O.)
* Correspondence: igor.sersa@ijs.si

Abstract: Wood is a widely used material because it is environmentally sustainable, renewable and relatively inexpensive. Due to the hygroscopic nature of wood, its physical and mechanical properties as well as the susceptibility to fungal decay are strongly influenced by its moisture content, constantly changing in the course of everyday use. Therefore, the understanding of the water state (free or bound) and its distribution at different moisture contents is of great importance. In this study, changes of the water state and its distribution in a beech sample while drying from the green (fresh cut) to the absolutely dry state were monitored by 1D and 2D ^{1}H NMR relaxometry as well as by spatial mapping of the relaxation times T_1 and T_2. The relaxometry results are consistent with the model of homogeneously emptying pores in the bioporous system with connected pores. This was also confirmed by the relaxation time mapping results which revealed the moisture transport in the course of drying from an axially oriented early- and latewood system to radial rays through which it evaporates from the branch. The results of this study confirmed that MRI is an efficient tool to study the pathways of water transport in wood in the course of drying and is capable of determining the state of water and its distribution in wood.

Keywords: magnetic resonance imaging (MRI); relaxation times; beech (*Fagus sylvatica*); wood; moisture content (MC)

Citation: Mikac, U.; Merela, M.; Oven, P.; Sepe, A.; Serša, I. MR Study of Water Distribution in a Beech (*Fagus sylvatica*) Branch Using Relaxometry Methods. *Molecules* **2021**, *26*, 4305. https://doi.org/10.3390/molecules26144305

Academic Editor: José A. González-Pérez

Received: 24 June 2021
Accepted: 13 July 2021
Published: 16 July 2021

1. Introduction

Wood is a hygroscopic porous and permeable material that is widely used in everyday life. It interacts with water from humid air causing a constantly changing moisture content (MC), especially in the outdoor use where it is exposed to dynamic moisture cycles. The MC changes affect the wood properties and are responsible for shrinkage and swelling of wood, moisture-induced stresses and mechanosorptive effects, which may lead to cracking or loss of loadbearing capacity. Wood contains macromolecules that link water by hydrogen bonding [1,2]. Thus, water in wood exists as bound and free water. Free water is in the form of liquid or vapor in cell lumina and bound water is hydrogen bonded in the cell wall material. Changed in the MC in the range between the absolutely dry wood (MC = 0%) and the wood at the fiber saturation point (FSP) (approximately 30%) where all water is bound in the cell walls cause alterations in physical and mechanical properties of wood. At higher MCs, water also exists as free water with almost no effect on the physical and mechanical properties. It is established that the optimal fungal growth is achieved at MC = 35–50% on the basis of dry weight. Therefore, the knowledge about the state of water and moisture transport in wood is of utmost importance for understanding its utilization, durability and wood product quality [3].

Different methods such as traditional gravimetrical determination, methods based on the electrical properties of moist wood and titration, for instance, are used to measure the MC of wood [4]. Among other methods, nuclear magnetic resonance (NMR) and

magnetic resonance imaging (MRI) have been successfully employed for studying the MC in wood [5–9] as well as its spatial distribution in wood samples [10–20]. The spin–lattice (T_1) and spin–spin (T_2) relaxation times of the protons in wood change with the MC. This is because the NMR relaxation times depend on the local environment of protons as they determine the mobility of molecules and thus influence the T_1/T_2 ratio. This ratio is higher in the environment with molecules of higher mobility [21]. The T_2 of protons in solid wood is in tens of microseconds, the T_2 of bound water with hindered local motion is in the range from hundreds of microseconds to several milliseconds, while the T_2 of free water in the cell lumina is in the range from tens to hundreds of milliseconds [6,22,23]. In addition, the T_2 values of free water depend on cell dimensions i.e., the T_2 of free water is longer in cells with larger lumina [24]. Therefore, four peaks are observed in the T_2 distribution of wood. The first two peaks are associated with free water and are therefore at higher T_2 values. Their amplitudes decrease with a decreasing MC and they vanish at MCs below the FSP. The third peak at shorter T_2 is associated with bound water. Its amplitude is constant with MCs above the FSP but it starts to decrease with MCs lower than the FSP. The fourth peak is associated with solid wood and it is at the shortest T_2 values. The amplitude of this peak is constant with any MC [6,13,22,25,26]. Different relaxation time values thus enable determination of the water state in the wood. The simplest are one-dimensional (1D) T_1 and T_2 spectra which enable distinction between bound and free water. More complex are two-dimensional (2D) T_1–T_2 and T_2–T_2 correlation spectra with which improvement of the resolution and information on water states in the wood is significant. T_1–T_2 correlation spectra enable distinction between the two types of bound water in cell walls, while T_2–T_2 correlation spectra can identify the water exchange between cell walls and the free water in the lumina, enabling measurement of the corresponding exchange rates [27]. These methods have also been used to study the adsorption mechanisms in earlywood and latewood [28], determine the structural changes of wood after thermal modification [29] and the effect of wood aging at the molecular level [9] and to characterize the decay process of wood due to fungal decomposition [30].

Proton density-weighted MRI produces a signal that is proportional to free water in wood, but it cannot detect bound states of water and solid wood. This is because the NMR signal of bound water and solid wood decays before detection with standard imaging methods. More precise information on the state of water in wood can be obtained from T_1, T_2 and apparent diffusion coefficient (ADC) maps [31]. T_2 maps are, in particular, important to get better contrast between free water in different wood structures [17,30].

The goal of this study is to demonstrate that NMR relaxometry is a powerful technique that allows studying the distribution and movement of water, free or bound, in different anatomical structures of wood in the course of its drying. Specifically, 1D T_1 and T_2 distributions, 2D T_1–T_2 correlation spectra and T_1 and T_2 maps of a beechwood sample at different MCs in the range from 90% (green state) to an absolutely dry sample were measured in this study to follow changes of the water state and distribution in the course of wood drying.

2. Results and Discussion

2.1. 1D T_1 and T_2 Distributions at Different MCs

A multiexponential analysis of T_1 and T_2 relaxation decay curves was used to determine the relaxation time distributions. Figure 1 shows the T_1 and T_2 distributions for different MCs. T_1 distributions consisted of two peaks: an intense peak in the range of hundreds of milliseconds and a small peak at few milliseconds. With the decreasing MC (wood drying), the position of the intense peak first decreased, reached a minimum value of 210 ms at MC = 25% and then increased with the decreasing MC (Figure 1a). The values of the shorter T_1 components were in the range of 10 ms. This peak was almost constant with drying until MC = 20% and then increased with a decreasing MC, up to 50 ms at MC = 9%. In the course of drying, the integrated intensities of both peaks slightly decreased until MC = 42%. Then, the integral of the longer T_1 component decreased and the integral of the

shorter T_1 component increased in the MC range between 42% and 20%, whereas at MCs below 20%, the integral of the longer component increased and the integral of the shorter component decreased and was no longer observed at MC = 0% (Figure 1a).

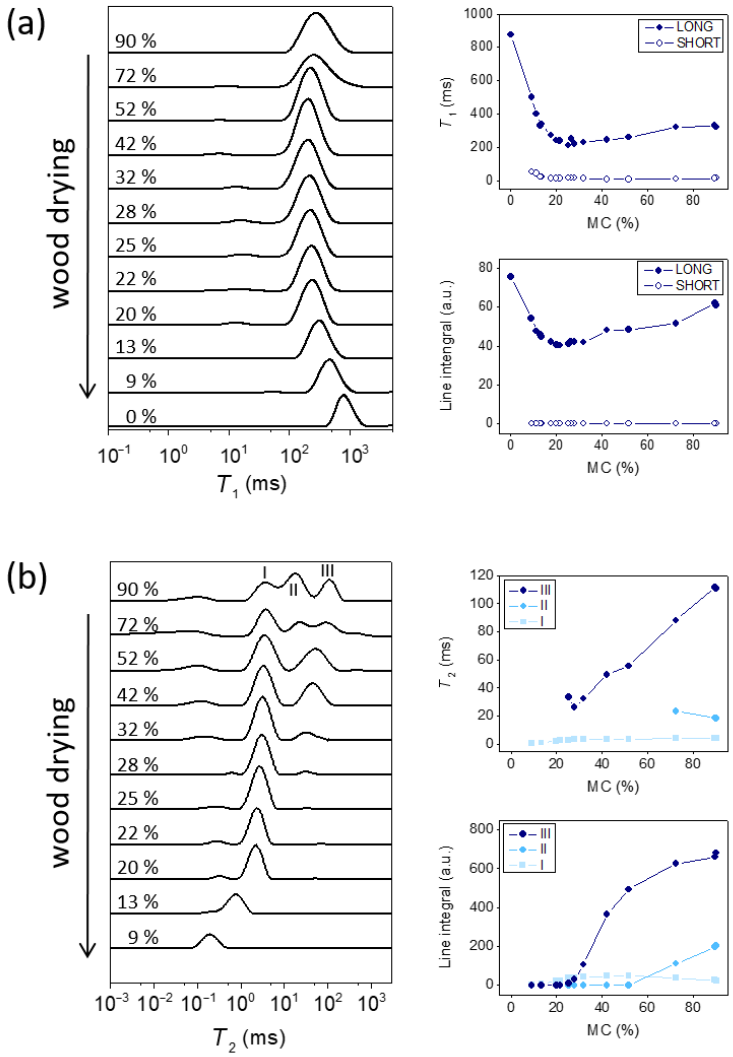

Figure 1. NMR relaxation time distributions together with the central relaxation time and the integrated intensities of the peaks at different MCs for the beech branchwood sample: (**a**) T_1 and (**b**) T_2. The labels LONG and SHORT in the graphs in panel (**a**) correspond to the T_1 values of an intense peak in the range of hundreds of milliseconds (long) and to a small peak at few milliseconds (short), while the labels I, II and III in the graphs in panel (**b**) correspond to short, medium and long T_2 values of three distinct peaks in T_2 distributions.

The T_2 distributions are, however, different (Figure 1b). A small and broad peak was observed in the T_2 distribution at 0.1 ms that remained almost constant throughout the sample drying. In addition, three peaks I, II and III were observed at higher MCs. With the decreasing MC (wood drying), peak I remained at the same position until MC = 20% and shifted to lower values at lower MCs. The T_2 of peak II slightly increased when MC decreased from 90% to 72% and then overlapped with peak III or I at lower MCs. Peak III shifted to lower values with the decreasing MC. The integrated intensity of peak I increased with the decreasing MC until 52%, remained constant until MC = 25% and decreased with MC further decreasing, while the integral of peak III decreased with the decreasing MC and was no longer observed at MCs lower than 25%. As in the previous studies [25,26,29,30,32–35], the peaks I, II and III were assigned to bound water, free water in cells with smaller lumina and free water in cells with larger lumina, respectively.

2.2. Two-Dimensional T_1–T_2 Correlation Spectra at Different MCs

To further evaluate the T_1 and T_2 results, 2D T_1–T_2 correlation spectra were measured for three different MCs (Figure 2). At MC = 90%, five peaks (labeled A1, A2, B, C and D, see Figure 2) were observed, with two different T_1 and four different T_2 values. The peaks A1, A2 and C were just below the diagonal $T_1 = T_2$, while the peaks B and C had similar T_2 but different T_1. The intensities and positions of the peaks kept changing with MC. At MC = 35%, intensities of the peaks A1 and A2 decreased significantly and could not be distinguished, and the intensity of peak C increases compared to its intensity at MC = 90%. At MC = 6%, the peaks A1 and A2 were no longer observed, and peak C had a very low intensity. The T_1 values of all the peaks decreased when the MC decreased from 90% to 35% and increased again when the MC decreased to 6%. Peaks B and C had similar T_2 values at MC = 90% and 35%; however, their T_2 values decreased at MC = 6%. The peaks in the T_1–T_2 correlation spectra could be identified on the basis of previous analyses [27]. The peaks with longer T_1 and the longest T_2 (A1 and A2) arose from water with the highest molecular mobility, i.e., free water in lumina with different diameters. Peak B with shorter T_2 corresponded to bound water, peak D with the shortest T_2—to solid-like protons. Peak C with shorter T_1 and the same T_2 as peak B was assigned to the water absorbed in wood polymers.

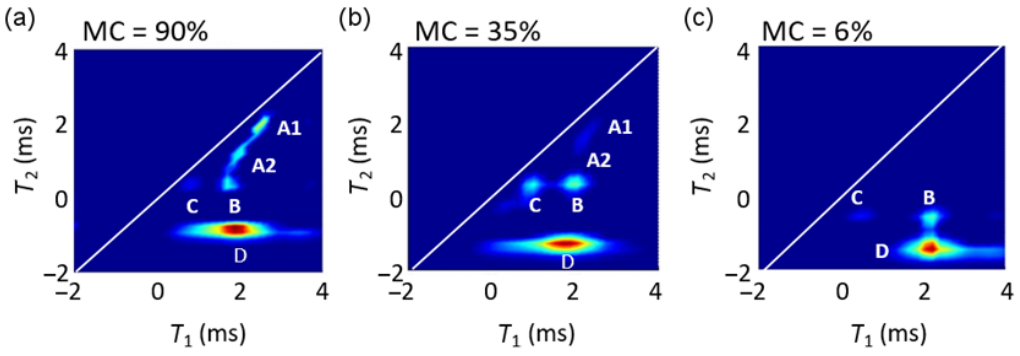

Figure 2. Two-dimensional T_1–T_2 correlation spectra of the beech branchwood sample at: (**a**) MC = 90%, (**b**) MC = 35% and (**c**) MC = 6%. The five peaks are attributed to free water in cell lumina (A1 and A2), protons of bound water (B and C) and solid wood protons (D) as discussed in the text.

2.3. MR Imaging: Proton Density Images and T_1 and T_2 Maps

The spatial distributions of relaxation times in the wood sample were measured by T_1 and T_2 mapping. For the proton density imaging, the first image with the shortest echo time of a sequence of echo images for T_2 map determination was used. It should be noted that the shortest echo time was still too long to allow detection of a signal from protons in solid wood as their T_2 values are in the range of tens of microseconds. The imaging method which was used allows detection of signals with T_2 values over a millisecond. For the same reason, the signal of bound water with T_2 of hundreds of microseconds produces a low signal that is, therefore, not completely detected. Thus, the signal of proton density images consists mainly of free water. Relaxation time maps were calculated by the complete set of echo images using the best fit to the monoexponential decaying function. The resolution of the images is lower than the size of a wood cell and therefore each pixel of the image consists of several cells with the cell lumina and cell walls. This implies that the multi-component decaying exponential function would yield a more accurate fit to the data and determine the relaxation times of all the states of water and solid protons in each pixel. However, due to the insufficient signal-to–noise ratio (SNR), the monoexponential fit was used. In addition, T_2 values measured using the spin-echo imaging pulse sequence at various echo times are underestimated due to diffusional loss of the signal during read gradients [31,36]. Therefore, the T_2 values cannot be directly compared to the spectroscopically determined

T_2 values, especially for protons with longer T_2 values. Nevertheless, the T_1 and T_2 maps can still give valuable information on the water in different wood structures.

Proton density images, T_1 and T_2 maps are shown in Figure 3. The brightness of these images is proportional to proton density, T_1 and T_2 relaxation times, respectively. The proton density image at MC = 90% shows different anatomical structures: annual rings with earlywood and latewood and rays. The annual rings and rays are also clearly shown on the T_1 and T_2 maps. It can be seen from the maps that both relaxation times were longer in the earlywood compared to the latewood and the shortest in the rays (Table 1). As the MC decreased, the contrast between different wood tissues increased. Signal intensity in the rays increased due to an increased amount of free water with longer T_2 relaxation time. In contrast, the signal of the annual rings decreased due to a decrease of free water amount as well as T_2 reduction in partially filled lumina. At MC = 32%, the rays were either filled with free water or already empty, which can be seen in the corresponding MR image and maps as indicated by high or no signal intensity.

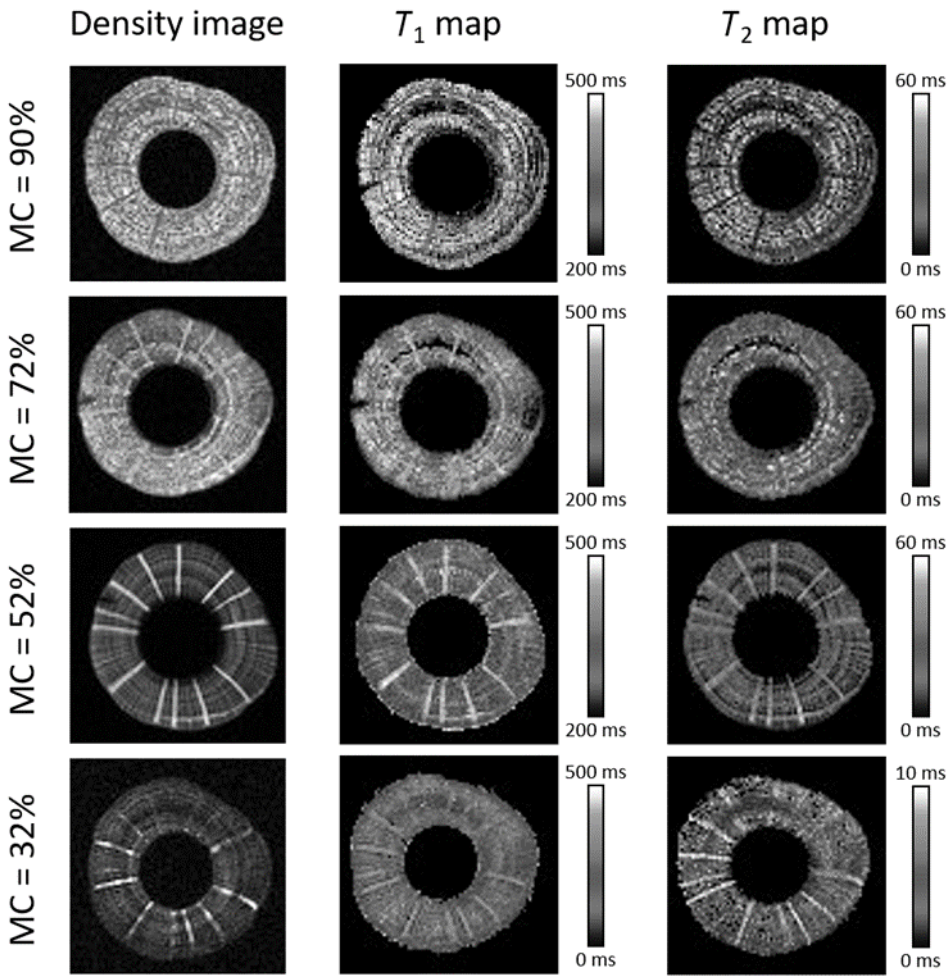

Figure 3. Density images, T_1 and T_2 maps of beech branchwood at different MCs. Note that the scales for the T_1 and T_2 maps are different for MC = 32% than for the higher MCs.

In some MR maps, a dark region with shorter T_1 and T_2 values or even with non-defined relaxation times values is observed due to too low SNR. It is interesting to note that the relaxation times of the rays in this region remained the same as for the rays elsewhere in the sample. This region is not observed in images at all the MCs because the sample was removed from the magnet after measurement at each MC, and the slices of the images at different MCs might be slightly different.

Table 1. T_1 and T_2 values of earlywood, latewood and ray regions obtained from the T_1 and T_2 maps at different MCs.

MC		T_1 (ms)	T_2 (ms)
90%	Earlywood	350 ± 30	35 ± 5
	Latewood	290 ± 20	17 ± 2
	Ray	290 ± 20	12 ± 2
72%	Earlywood	330 ± 30	30 ± 5
	Latewood	300 ± 20	17 ± 2
	Ray	400 ± 20	27 ± 2
52%	Earlywood	320 ± 30	24 ± 3
	Latewood	260 ± 20	13 ± 2
	Ray	400 ± 20	35 ± 2
32%	Earlywood	230 ± 30	5 ± 1
	Latewood	180 ± 20	3 ± 1
	Ray	280 ± 20	8 ± 1

2.4. Discussion

Wood contains two main proton compartments: solid wood material (cellulose, hemicellulose and lignin) and water that can be observed in cell cavities as lumen water (free water) or bound in cell walls (bound water). It should be noted that the relaxation times of lumen water depend on the cell size [1]. Since wood generally contains a continuous distribution of cell sizes, the analysis of relaxation time distributions using inverse Laplace transformation (LT) is more appropriate than a multiexponential analysis using a model function equal to the sum of a predefined number of exponentially decaying functions. In the study, 1D inverse Laplace transformation was applied to the experimental data obtained by the inversion recovery (IR) and Carr–Purcell–Meiboom–Gill (CPMG) pulse sequences to calculate 1D distributions (spectra) of the T_1 and T_2 relaxations times, respectively. The drawback of the 1D LT relaxation time distribution analysis is that it cannot always resolve all different proton compartments in wood, particularly in cases when different proton compartments have similar T_1 or T_2 values and the spectral peaks overlap. However, if these protons have similar T_2 but different T_1 values or vice versa, then it is possible to resolve these different proton compartments by 2D T_1–T_2 correlation spectroscopy. This was performed using 2D LT of the data acquired by the IR–CPMG sequence. Two-dimensional T_1–T_2 correlation spectra were measured at three different MCs in order to differentiate the overlapping peaks in the 1D relaxation time spectra. To obtain differences in relaxation times for different wood structures, 2D T_1 and T_2 maps were measured as well.

The T_1 distributions had two peaks (Figure 1a). The two peaks in the T_1 distributions were attributed to different T_1 values of earlywood and latewood in red cedar and hemlock [37] or the fast exchange between free and bound water [25,27]. Results of the T_1 maps (Figure 3, Table 1) yielded values in the earlywood, latewood and ray regions in the range of the longer T_1 component, i.e., 100–700 ms. These results are therefore more consistent with the fast exchange scenario.

Differences in the T_2 distributions (Figure 1b) in the course of sample drying show that T_2 and integrated intensity of peak III decreased with the decreasing MC and the peak vanished at MC = 25%. This value is close to that of the FSP where all free water evaporates and only bound water remains. Peak III can therefore be assigned to free water in cell lumina. Peak II could not be distinguished from peaks I and III at MCs below 72%. It is interesting to note that the T_2 value of peak II increased when MC decreased from 90% to 72%. In the previous studies, these two peaks were associated with free water in cell lumina of different sizes [25,29,32–35] as the T_2 value is directly proportional to the pore size [24]. Peak III was assigned to free water in earlywood vessels, peak II—to free water in smaller latewood vessels and ray cells. Another study suggested that peak III corresponds to free water in tracheid (fiber) cells, peak II—to free water in ray cell lumina, pits and tracheid lumen ends [32]. The T_2 value of peak I was constant down to MC = 20% (just below the FSP) and then decreased with the decreasing MC. The dependence of the integrated line

intensity of peak I on MC is interesting. The integrated intensity first increased, then it was constant and finally decreased again below MC = 20%. This can be explained by the model of a bioporous system with connected pores [38]. The T_2 value and the integrated intensity of peak III decreased in the course of drying indicating the homogeneous decrease of water in large pores. The increase in the integrated intensity of peak I shows that the larger and smaller pores were connected, and emptying of the large pores left some liquid films along the walls. The water of the liquid film has a much shorter T_2 that could overlap with the T_2 values of the smaller pores or even with the T_2 values of bound water. This result was also supported by the T_1–T_2 correlation spectra (Figure 2) where two peaks with different T_2 values and an identical T_1 value were observed, i.e., peaks B and C. The intensity of peak C, i.e., the bound water with higher mobility (higher T_1/T_2) increased as the MC decreased from 90% to 35% than the bound water assigned to peak B (lower T_1/T_2), At MC = 35%, almost no free water was in the cell lumina (low intensity of the peaks A1 and A2). This result can be explained by an increasing proportion of liquid film on cell walls with decreasing MCs (wood drying). The signal of the liquid film can be assigned to the peak of bound water with higher mobility (peak C). With further drying of the sample below the FSP, the intensity of peak C decreased while the intensity of peak B was almost the same, i.e., highly mobile bound water evaporates first, causing the decrease of peak II at MCs below 20%.

In addition to three peaks (I, II and III) in the T_2 distribution, there was also a peak at much shorter T_2 values of around 100 µs corresponding to peak D in the T_1–T_2 correlation spectra. This peak remained constant throughout drying of the sample and was assigned to solid wood. However, the T_2 values of the solid wood are in the range of several tens of microseconds. This is too short for signal detection with the CPMG sequence at the parameters used in this study. Thus, most probably only the part of the spectrum with the longest T_2 values of solid wood was successfully measured while the actual T_2 of this peak was below our detection limit.

The spatial distribution of the T_2 value at various MCs is shown in T_2 maps (Figure 3 and Table 1). Shorter T_2 value for latewood than for earlywood at all MCs was observed, which is in agreement with a previous study [17] and is the consequence of larger lumina of earlywood cells compared to latewood cells. The T_2 value of the rays first increased with the MC decrease down to 52%. At this MC, the T_2 value of the ray tissue was even higher than the T_2 value of earlywood. As the MC decreased to 32%, the T_2 value of rays decreased as well but was still higher than the T_2 value of larger earlywood vessels at this MC. The multiseriate rays were larger than the earlywood vessels. Therefore, an additional reason for the longer T_2 value was a higher amount of water in ray cells; namely, the T_2 value increased with the water concentration in pores [38]. These results indicate that in the course of drying of a wood sample, water is diffused from the annual rings to the rays before evaporating from the sample. The spatial distribution of the T_2 value at different MCs can also explain vanishing of peak II below MC = 72%, i.e., high above the FSP. The T_2 value of the ray cells at high MC contributed to peak II. As the ray cells were filled with more water at lower MCs, the T_2 of free water in the cells increased and began to overlap with the T_2 value of peak III. Free water in latewood cells also contributed to peak II at high MCs. However, as the amount of water decreased in the course of drying, the T_2 value of the latewood decreased to several milliseconds such that the T_2 value of free water in partially empty latewood cells could overlap with peak I.

This study was performed on small samples due to the sample size limitations of the MRI scanner that was used in the study. The scanner was optimized for spatial resolution (for MR microscopy) and therefore had very sensitive but small RF probes. The largest RF probe had a diameter of only 27 mm and this was also the largest sample size that could be scanned. However, the identical methodology used in this study can be used on a much larger scale, e.g., with clinical scanners, where the samples can be up to ten times larger than in this study.

3. Materials and Methods

3.1. Plant Material

Five 15-mm-long samples of a young forest beech tree (*Fagus sylvatica L.*) were cut from fresh branches with a diameter of approximately 8 mm and the annual growth ring width of 0.2 mm. Pith and bark were removed from the samples to avoid large variations of MCs in the samples. The samples were then dried in a desiccator until the MC of the samples decreased from the initial 88% (in the green state) to below 20%. This was needed in order to reach the state of wood below the fiber saturation point (FSP) with only bound water. To moisten the samples to different well-defined MCs, they were equilibrated in a desiccator over different salt solutions ensuring different relative air humidities (RH): $MgCl_2$ (RH = 33%), K_2CO_3 (RH = 44%), $NaNO_2$ (RH = 65%), NaCl (RH = 75%), and $ZnSO_4$ (RH = 85%). After all the MR experiments were finished, the samples were completely dried in the oven at 103 °C for several hours until their masses were equilibrated. The MCs were determined gravimetrically using the Equation (1).

$$\mathrm{MC} = \frac{m - m_0}{m_0} \times 100\% \quad (1)$$

where m is the mass of a moist sample and m_0 is the mass of an absolutely dry sample. Wood density in the absolutely dry state was 580 kg/m^3.

3.2. NMR and MRI Experiments

The NMR and MRI experiments were performed on a system consisting of a superconducting 2.35-T (^{1}H NMR frequency of 100 MHz) horizontal bore magnet (Oxford Instruments, Abingdon, UK) equipped with gradients and RF coils for MR microimaging (Bruker, Ettlingen, Germany) using a Tecmag Apollo (Tecmag, Houston, TX, USA) NMR/MRI spectrometer. For the MR experiments, the wood sample was taken out of the desiccator at appropriate time intervals, weighted and inserted into a glass tube that was sealed with a Teflon cap to prevent sample drying during the scanning. The sample was reoriented in the magnet in such a way that it allowed the imaging of an axial slice (parallel to the radial–tangential plane) in 2D MRI experiments. Each sample was weighted before and after the MR measurements. The maximal change of weight during MR experiments was less than 2% and observed only for the samples with high MC, while the mass differences were negligible for the samples with MCs less than 30%.

The spin–spin relaxation times T_2 were measured using the Carr–Purcell–Meiboom–Gill (CPMG) sequence 90°–τ–[180°–τ–AQ–τ]^N with the echo time τ of 150 μs and loop repetitions N of 3000 in order to enable measurement of a wide range of T_2 values for the sample with different MCs. To measure the spin–lattice relaxation time T_1, the inversion recovery (IR) pulse sequence 180°–τ_1–90°–AQ was used, with the logarithmically increasing IR delay τ_1 (from 20 μs to 10 s; 36 different τ_1 values). To further validate the relaxation results, 2D T_1–T_2 relaxation correlations were measured at three different MCs, 90%, 35% and 6%, using the IR-CPMG sequence, where the IR part was followed by the CPMG loop [39]. The IR delays were the same as for 1D T_1 measurements. The echo delays in the CPMG loop were equal to 350 μs, 50 μs and 25 μs, with the number of loops of 2048, 1024 and 512 for the samples with the MC of 90%, 35% and 6%, respectively.

The experimental data of T_1, T_2 and T_1–T_2 measurements were processed via a multiexponential analysis using the Prospa software that was provided by Prof. P. Callaghan [36,39]. The analysis based on multidimensional inverse Laplace transformation allows the resolution and quantification of various components in the relaxation distribution to some extent.

Two-dimensional T_1 and T_2 relaxation time maps were measured using a modified spin-echo imaging pulse sequence. Specifically, the inversion recovery spin-echo (IR-SE) imaging sequence was used for T_1 mapping, i.e., a hard 180° pulse followed by the time interval τ_1 added before the standard 2D spin-echo imaging sequence. T_1 maps were determined from the IR-SE images measured with the time interval τ_1 ranging from 40 μs to 10 s (nine different τ_1 values); the echo time was equal to TE = 3.6 ms and the repetition

time was TR = 10 s. T_2 maps were determined from the standard 2D spin-echo images measured with the echo time (TE) varying between 3.6 ms (the shortest possible TE) and 300 ms (nine different values). The other imaging parameters for 2D images were as follows: field of view (FOV) = 13 mm, matrix size of 128 × 128 and slice thickness = 1 mm with the in-plane resolution of 0.1 mm. Proton density-weighted images were selected as the images with the shortest echo time (TE = 3.6 ms) of the sequence used for T_2 map calculation.

4. Conclusions

The present study demonstrates that a combination of 1D T_1 and T_2 spectra, 2D T_1–T_2 correlation spectra and their spatial distributions given by the T_1 and T_2 maps provides valuable information about changes in wood in the course of drying. The obtained results enabled precise analysis of moisture redistribution in the course of drying between different anatomic regions of wood. It also enabled determination of the ratio between the amounts of bound and free water as well as the amount of water in wood cells of different lumina. The advantage of the proposed method is also that it is non-destructive, non-invasive and non-contact and therefore enables MC analysis of the same sample during different stages of its drying.

Author Contributions: U.M., M.M., P.O., A.S. and I.S. conceived and designed the experiments; M.M. provided the samples; U.M., A.S. and I.S. performed the experiments; U.M. analyzed the data; U.M. wrote the original draft; M.M., P.O. and I.S. reviewed and edited the manuscript. All authors discussed the results and commented on the manuscript. All authors have read and agreed to the published version of the manuscript.

Funding: This research was funded by the Slovenian Research Agency through the Research Core Funding (Nos. P1-0060, P4-0015 and J1-7042).

Institutional Review Board Statement: Not applicable.

Informed Consent Statement: Not applicable.

Data Availability Statement: The data presented in this study are available on request from the corresponding author.

Acknowledgments: The authors thank Kanza Awais for proofreading an earlier version of the manuscript.

Conflicts of Interest: The authors declare no conflict of interest.

Sample Availability: Not available.

References

1. Bowyer, J.L.; Shmulsky, R.; Haygreen, J.G. *Forest Products and Wood Science*; Blackwell Publishing Professional: Ames, IA, USA, 2007.
2. Rostom, L.; Care, S.; Courtier-Murias, D. Analysis of water content in wood material through 1D and 2D H-1 NMR relax-ometry: Application to the determination of the dry mass of wood. *Magn. Reson. Chem.* **2021**, *59*, 614–627. [CrossRef]
3. Skaar, C. *Wood-Water Relations*; Springer Science and Business Media LLC: Berlin, Germany, 1988.
4. Dietsch, P.; Franke, S.; Franke, B.; Gamper, A.; Winter, S. Methods to determine wood moisture content and their applicability in monitoring concepts. *J. Civ. Struct. Health* **2015**, *5*, 115–127. [CrossRef]
5. Merela, M.; Oven, P.; Serša, I.; Mikac, U. A single point NMR method for an instantaneous determination of the moisture content of wood. *Holzforschung* **2009**, *63*, 348–351. [CrossRef]
6. Menon, R.; Mackay, A.L.; Hailey, J.R.T.; Bloom, M.; Burgess, A.E.; Swanson, J.S. An NMR determination of the physiological water distribution in wood during drying. *J. Appl. Polym. Sci.* **1987**, *33*, 1141–1155. [CrossRef]
7. Hartley, I.; Kamke, F.A.; Peemoeller, H. Absolute Moisture Content Determination of Aspen Wood Below the Fiber Saturation Point using Pulsed NMR. *Holzforschung* **1994**, *48*, 474–479. [CrossRef]
8. Thygesen, L.G. PLS calibration of pulse NMR free induction decay for determining moisture content and basic density of softwood above fiber saturation. *Holzforschung* **1996**, *50*, 434–436.
9. Rostom, L.; Courtier-Murias, D.; Rodts, S.; Care, S. Investigation of the effect of aging on wood hygroscopicity by 2D 1H NMR relaxometry. *Holzforschung* **2019**, *74*, 400–411. [CrossRef]
10. Bucur, V. *Nondestructive Characterization and Imaging of Wood*; Springer Science and Business Media LLC: Berlin, Germany, 2003.
11. Merela, M.; Oven, P.; Sepe, A.; Serša, I. Three-dimensional in vivo magnetic resonance microscopy of beech (*Fagus sylvatica* L.) wood. *Magma Magn. Reson. Mater. Phys. Biol. Med.* **2005**, *18*, 171–174. [CrossRef]

12. Brownstein, K. Diffusion as an explanation of observed NMR behavior of water absorbed on wood. *J. Magn. Reson. (1969)* **1980**, *40*, 505–510. [CrossRef]
13. Araujo, C.D.; Mackay, A.L.; Hailey, J.R.T.; Whittall, K.P.; Le, H. Proton Magnetic-Resonance Techniques for Character-ization of Water in Wood—Application to White Spruce. *Wood Sci. Technol.* **1992**, *26*, 101–113. [CrossRef]
14. Araujo, C.D.; Mackay, A.L.; Whittall, K.P.; Hailey, J.R.T. A Diffusion-Model for Spin-Spin Relaxation of Compart-mentalized Water in Wood. *J. Magn. Reson. Ser. B* **1993**, *101*, 248–261. [CrossRef]
15. Oven, P.; Merela, M.; Mikac, U.; Serša, I. 3D magnetic resonance microscopy of a wounded beech branch. *Holzforschung* **2008**, *62*, 322–328. [CrossRef]
16. Oven, P.; Merela, M.; Mikac, U.; Serša, I. Application of 3D magnetic resonance microscopy to the anatomy of woody tissues. *IAWA J.* **2011**, *32*, 401–414. [CrossRef]
17. Javed, M.A.; Kekkonen, P.M.; Ahola, S.; Telkki, V.-V. Magnetic resonance imaging study of water absorption in thermally modified pine wood. *Holzforschung* **2015**, *69*, 899–907. [CrossRef]
18. Žlahtič, M.; Mikac, U.; Serša, I.; Merela, M.; Humar, M. Distribution and penetration of tung oil in wood studied by magnetic resonance microscopy. *Ind. Crops Prod.* **2017**, *96*, 149–157. [CrossRef]
19. Zupanc, M.Ž.; Mikac, U.; Serša, I.; Merela, M.; Humar, M. Water distribution in wood after short term wetting. *Cellulose* **2018**, *26*, 703–721. [CrossRef]
20. Almeida, G.; Leclerc, S.; Perre, P. NMR imaging of fluid pathways during drainage of softwood in a pressure membrane chamber. *Int. J. Multiph. Flow* **2008**, *34*, 312–321. [CrossRef]
21. Abragam, A. *The Principles of Nuclear Magnetism*; Clarendon Press: Oxford, UK, 1961.
22. Almeida, G.; Gagné, S.; Hernández, R.E. A NMR study of water distribution in hardwoods at several equilibrium moisture contents. *Wood Sci. Technol.* **2006**, *41*, 293–307. [CrossRef]
23. Dvinskikh, S.; Henriksson, M.; Berglund, L.; Furó, I. A multinuclear magnetic resonance imaging (MRI) study of wood with adsorbed water: Estimating bound water concentration and local wood density. *Holzforschung* **2011**, *65*, 103–107. [CrossRef]
24. Brownstein, K.R.; Tarr, C.E. Importance of classical diffusion in NMR studies of water in biological cells. *Phys. Rev. A* **1979**, *19*, 2446–2453. [CrossRef]
25. Telkki, V.-V.; Yliniemi, M.; Jokisaari, J. Moisture in softwoods: Fiber saturation point, hydroxyl site content, and the amount of micropores as determined from NMR relaxation time distributions. *Holzforschung* **2013**, *67*, 291–300. [CrossRef]
26. Elder, T.; Houtman, C. Time-domain NMR study of the drying of hemicellulose extracted aspen (*Populus tremuloides* Michx.). *Holzforschung* **2013**, *67*, 405–411. [CrossRef]
27. Cox, J.; McDonald, P.J.; Gardiner, B. A study of water exchange in wood by means of 2D NMR relaxation correlation and exchange. *Holzforschung* **2010**, *64*, 259–266. [CrossRef]
28. Bonnet, M.; Courtier-Murias, D.; Faure, P.; Rodts, S.; Care, S. NMR determination of sorption isotherms in earlywood and latewood of Douglas fir. Identification of bound water components related to their local environment. *Holzforschung* **2017**, *71*, 481–490. [CrossRef]
29. Cai, C.; Javed, M.A.; Komulainen, S.; Telkki, V.-V.; Haapala, A.; Heräjärvi, H. Effect of natural weathering on water absorption and pore size distribution in thermally modified wood determined by nuclear magnetic resonance. *Cellulose* **2020**, *27*, 4235–4247. [CrossRef]
30. Hiltunen, S.; Mankinen, A.; Javed, M.A.; Ahola, S.; Venäläinen, M.; Telkki, V.-V. Characterization of the decay process of Scots pine caused by *Coniophora puteana* using NMR and MRI. *Holzforschung* **2020**, *74*, 1021–1032. [CrossRef]
31. Callaghan, P. *Principles of Nuclear Magnetic Resonance Microscopy*; Oxford University Press: New York, NY, USA, 1991.
32. Fredriksson, M.; Thygesen, L.G. The states of water in Norway spruce (*Picea abies* (L.) Karst.) studied by low-field nuclear magnetic resonance (LFNMR) relaxometry: Assignment of free-water populations based on quantitative wood anatomy. *Holzforschung* **2017**, *71*, 77–90. [CrossRef]
33. Xu, K.; Lu, J.; Gao, Y.; Wu, Y.; Li, X. Determination of moisture content and moisture content profiles in wood during drying by low-field nuclear magnetic resonance. *Dry. Technol.* **2017**, *35*, 1909–1918. [CrossRef]
34. Gezici-Koç, Ö.; Erich, S.J.F.; Huinink, H.P.; Van Der Ven, L.G.J.; Adan, O.C.G. Bound and free water distribution in wood during water uptake and drying as measured by 1D magnetic resonance imaging. *Cellulose* **2017**, *24*, 535–553. [CrossRef]
35. Xu, K.; Yuan, S.; Gao, Y.; Wu, Y.; Zhang, J.; Li, X.; Lu, J. Characterization of moisture states and transport in MUF resin-impregnated poplar wood using low field nuclear magnetic resonance. *Dry. Technol.* **2020**, *39*, 791–802. [CrossRef]
36. Godefroy, S.; Callaghan, P. 2D relaxation/diffusion correlations in porous media. *Magn. Reson. Imaging* **2003**, *21*, 381–383. [CrossRef]
37. Xu, Y.; Araujo, C.; Mackay, A.; Whittall, K. Proton Spin–Lattice Relaxation in Wood—T_1Related to Local Specific Gravity Using a Fast-Exchange Model. *J. Magn. Reson. Ser. B* **1996**, *110*, 55–64. [CrossRef]
38. Lerouge, T.; Maillet, B.; Coutier-Murias, D.; Grande, D.; Le Droumaguet, B.; Pitois, O.; Coussot, P. Drying of a Compressible Biporous Material. *Phys. Rev. Appl.* **2020**, *13*, 044061. [CrossRef]
39. Song, Y.-Q.; Venkataramanan, L.; Hurlimann, M.; Flaum, M.; Frulla, P.; Straley, C. T_1–T_2 Correlation Spectra Obtained Using a Fast Two-Dimensional Laplace Inversion. *J. Magn. Reson.* **2002**, *154*, 261–268. [CrossRef] [PubMed]